# Impact of low-frequency coding variants on human facial shape

Dongjing Liu[1], Nora Alhazmi[2,3], Harold Matthews[4,5], Myoung Keun Lee[6], Jiarui Li[7], Jacqueline T. Hecht[8], George L. Wehby[9], Lina M. Moreno[10], Carrie L. Heike[11], Jasmien Roosenboom[6], Eleanor Feingold[1,12], Mary L. Marazita[1,6], Peter Claes[4,7], Eric C. Liao[13], Seth M. Weinberg[1,6*], John R. Shaffer[1,6*]

## Supplementary Figures

**Fig S1. Implicated genes across broad facial regions from recent GWAS of common genetic variants (White et al. 2020 [1])**

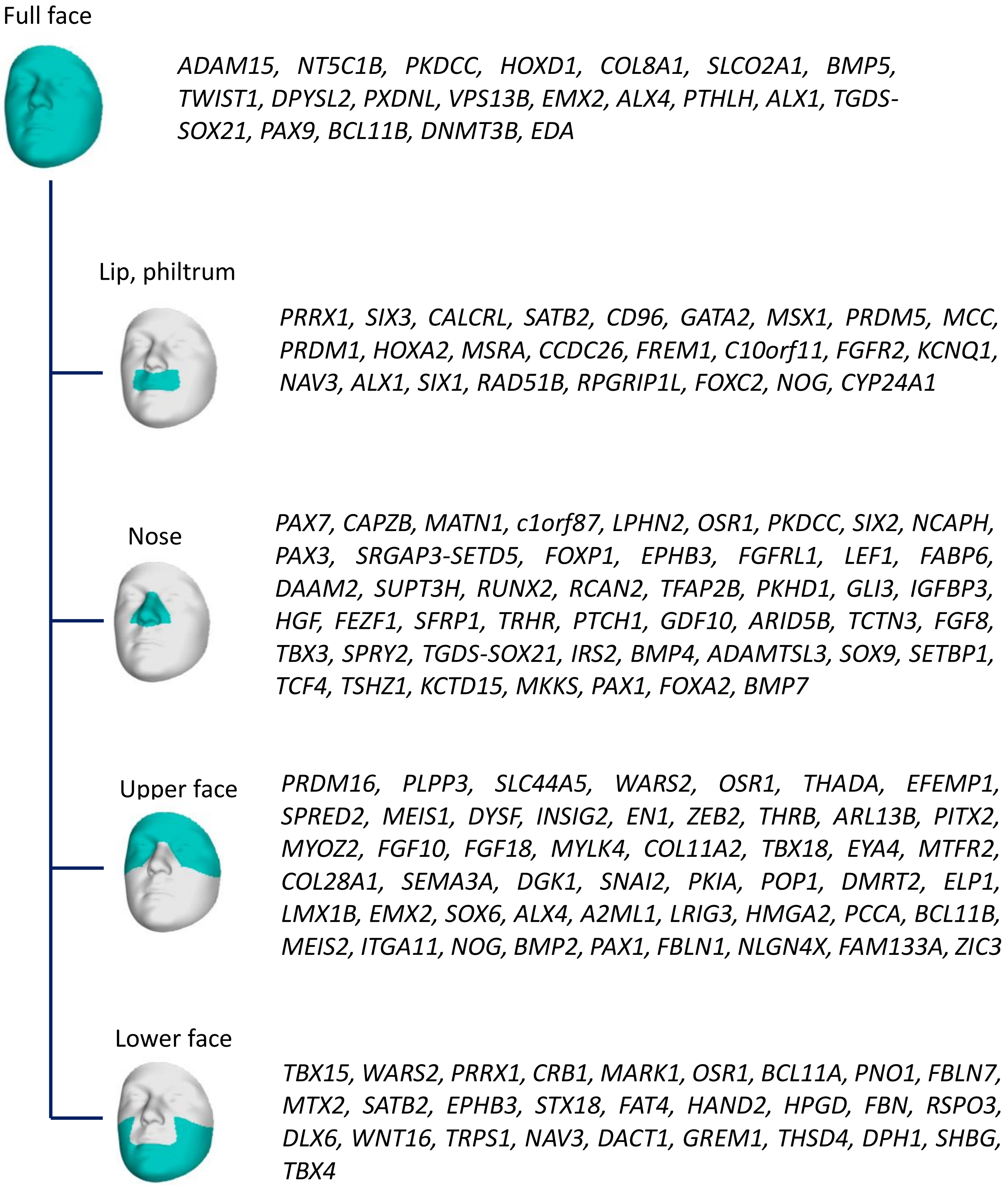

**Full face**

*ADAM15, NT5C1B, PKDCC, HOXD1, COL8A1, SLCO2A1, BMP5, TWIST1, DPYSL2, PXDNL, VPS13B, EMX2, ALX4, PTHLH, ALX1, TGDS-SOX21, PAX9, BCL11B, DNMT3B, EDA*

**Lip, philtrum**

*PRRX1, SIX3, CALCRL, SATB2, CD96, GATA2, MSX1, PRDM5, MCC, PRDM1, HOXA2, MSRA, CCDC26, FREM1, C10orf11, FGFR2, KCNQ1, NAV3, ALX1, SIX1, RAD51B, RPGRIP1L, FOXC2, NOG, CYP24A1*

**Nose**

*PAX7, CAPZB, MATN1, c1orf87, LPHN2, OSR1, PKDCC, SIX2, NCAPH, PAX3, SRGAP3-SETD5, FOXP1, EPHB3, FGFRL1, LEF1, FABP6, DAAM2, SUPT3H, RUNX2, RCAN2, TFAP2B, PKHD1, GLI3, IGFBP3, HGF, FEZF1, SFRP1, TRHR, PTCH1, GDF10, ARID5B, TCTN3, FGF8, TBX3, SPRY2, TGDS-SOX21, IRS2, BMP4, ADAMTSL3, SOX9, SETBP1, TCF4, TSHZ1, KCTD15, MKKS, PAX1, FOXA2, BMP7*

**Upper face**

*PRDM16, PLPP3, SLC44A5, WARS2, OSR1, THADA, EFEMP1, SPRED2, MEIS1, DYSF, INSIG2, EN1, ZEB2, THRB, ARL13B, PITX2, MYOZ2, FGF10, FGF18, MYLK4, COL11A2, TBX18, EYA4, MTFR2, COL28A1, SEMA3A, DGK1, SNAI2, PKIA, POP1, DMRT2, ELP1, LMX1B, EMX2, SOX6, ALX4, A2ML1, LRIG3, HMGA2, PCCA, BCL11B, MEIS2, ITGA11, NOG, BMP2, PAX1, FBLN1, NLGN4X, FAM133A, ZIC3*

**Lower face**

*TBX15, WARS2, PRRX1, CRB1, MARK1, OSR1, BCL11A, PNO1, FBLN7, MTX2, SATB2, EPHB3, STX18, FAT4, HAND2, HPGD, FBN, RSPO3, DLX6, WNT16, TRPS1, NAV3, DACT1, GREM1, THSD4, DPH1, SHBG, TBX4*

[1] White,J.D., Indencleef,K., Naqvi,S., Eller,R.J., Hoskens,H., Roosenboom,J., Lee,M.K., Li,J., Mohammed,J., Richmond,S., *et al.* (2020) Insights into the genetic architecture of the human face. *Nat Genet*, **66**, 101–9.

**Fig S2. Q-Q plot of gene-based MultiSKAT tests by facial module.** Genomic inflation factor λ is shown at the top left corner of each subfigure. There was little evidence for systematic inflation in p-values.

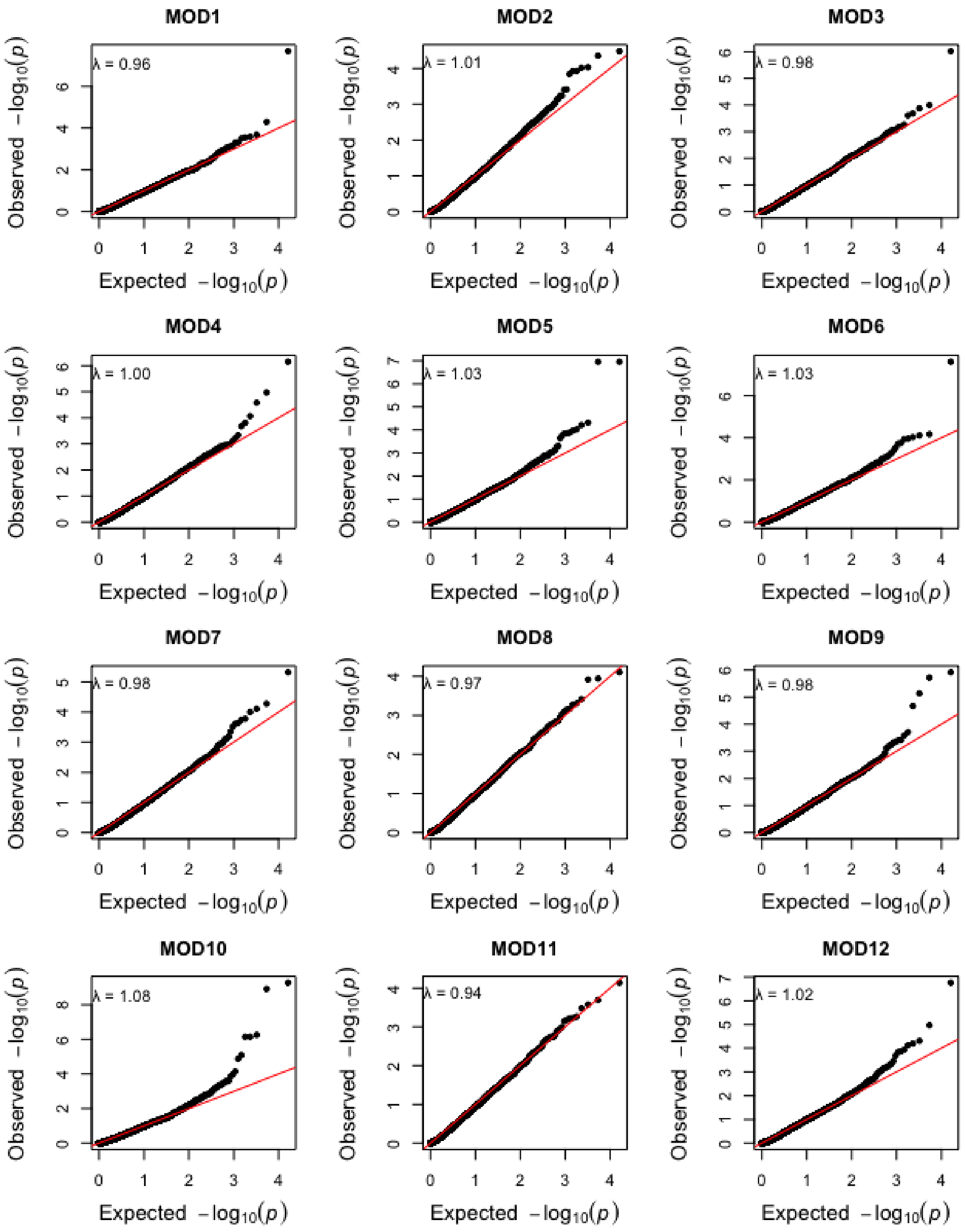

**Fig S2. Q-Q plot of gene-based MultiSKAT tests by facial module (Cont)**

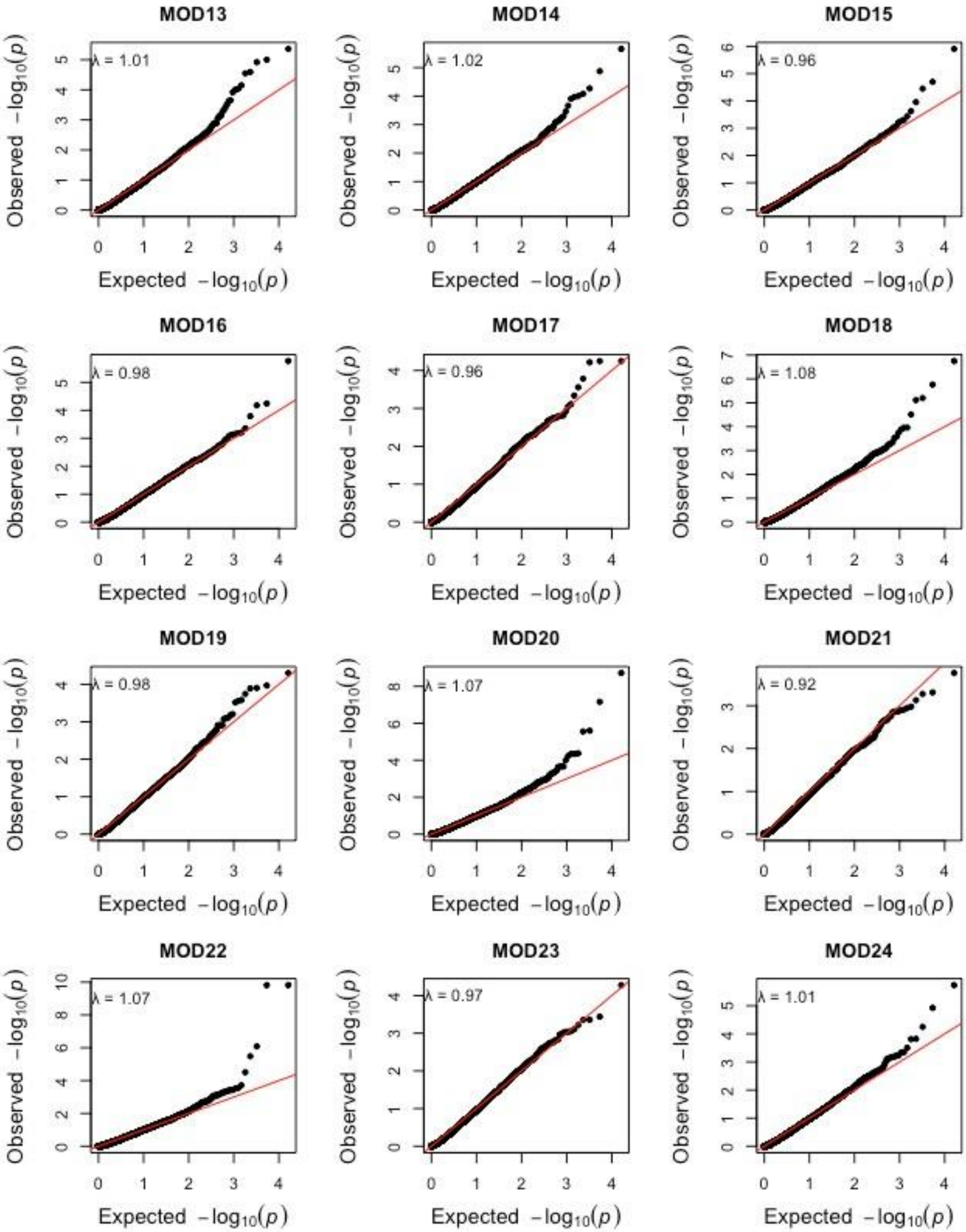

**Fig S2. Q-Q plot of gene-based MultiSKAT tests by facial module (Cont)**

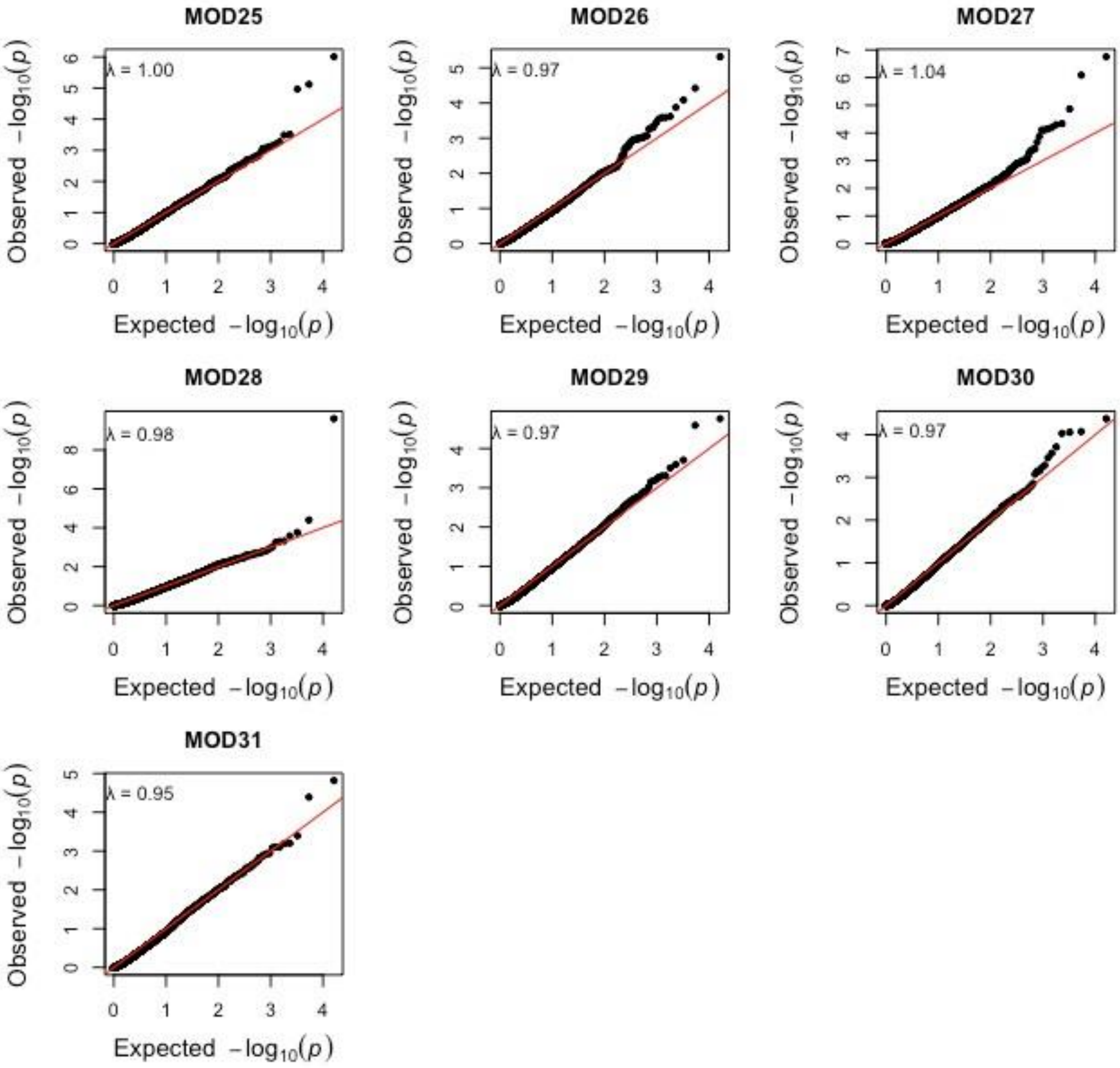

## Fig S3. FUMA enrichment results

a) GO biological process

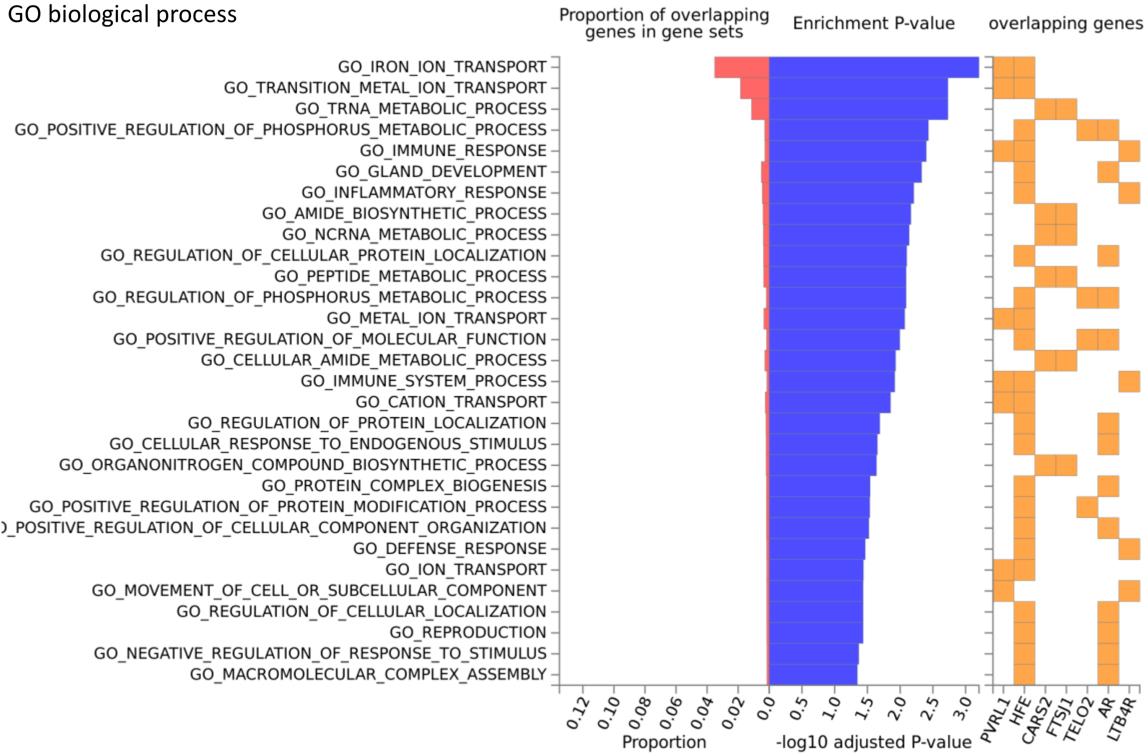

b) GO molecular function

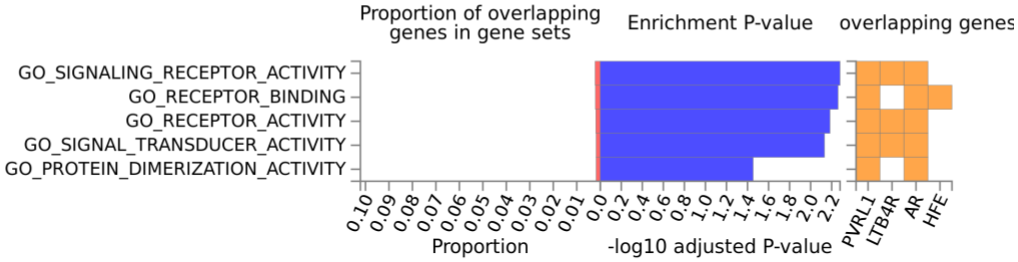

c) GWAS catalog

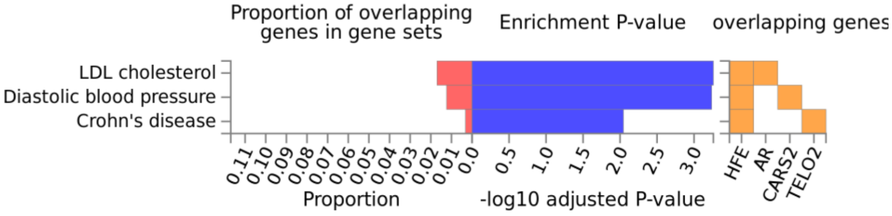

**Fig S4. GTEx expression of MultiSKAT significant genes in tissues relevant to facial morphology.** Dendrogram denotes similarity in expression level. TPM, transcripts per million

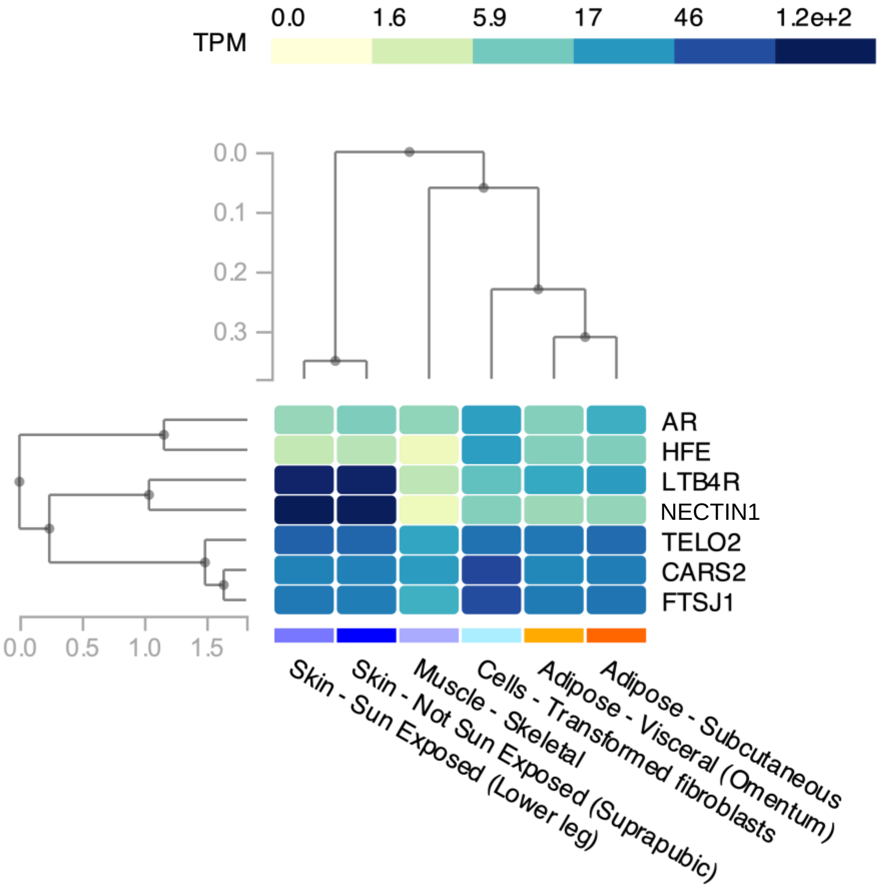

**Fig S5. Magnitude of variant effect on facial modules, quantified by the Euclidean distance between averaged faces of different genotype groups.** The 95% confidence interval was obtained by 5000 bootstraps. The farther away the blue (common) or red (low-freq) rectangular boxes fall from line x=0, the larger the group distances and the greater the magnitude of effects. Common variants that yielded significant GWAS association in the same cohort with the same modules are used as a comparison to low-frequency variants. Genotype groups column indicates the two groups of people of whom the faces were averaged and distance was computed. For example, 0 vs 1/2 means major allele homozygotes vs the remaining. The following two columns indicate sizes of the two groups in comparison. Low-frequency variants had large effects compared to previously reported common variants, although this could be a result from the much smaller size of carrier group and may not reflect genuine greater effects of low-frequency variants.

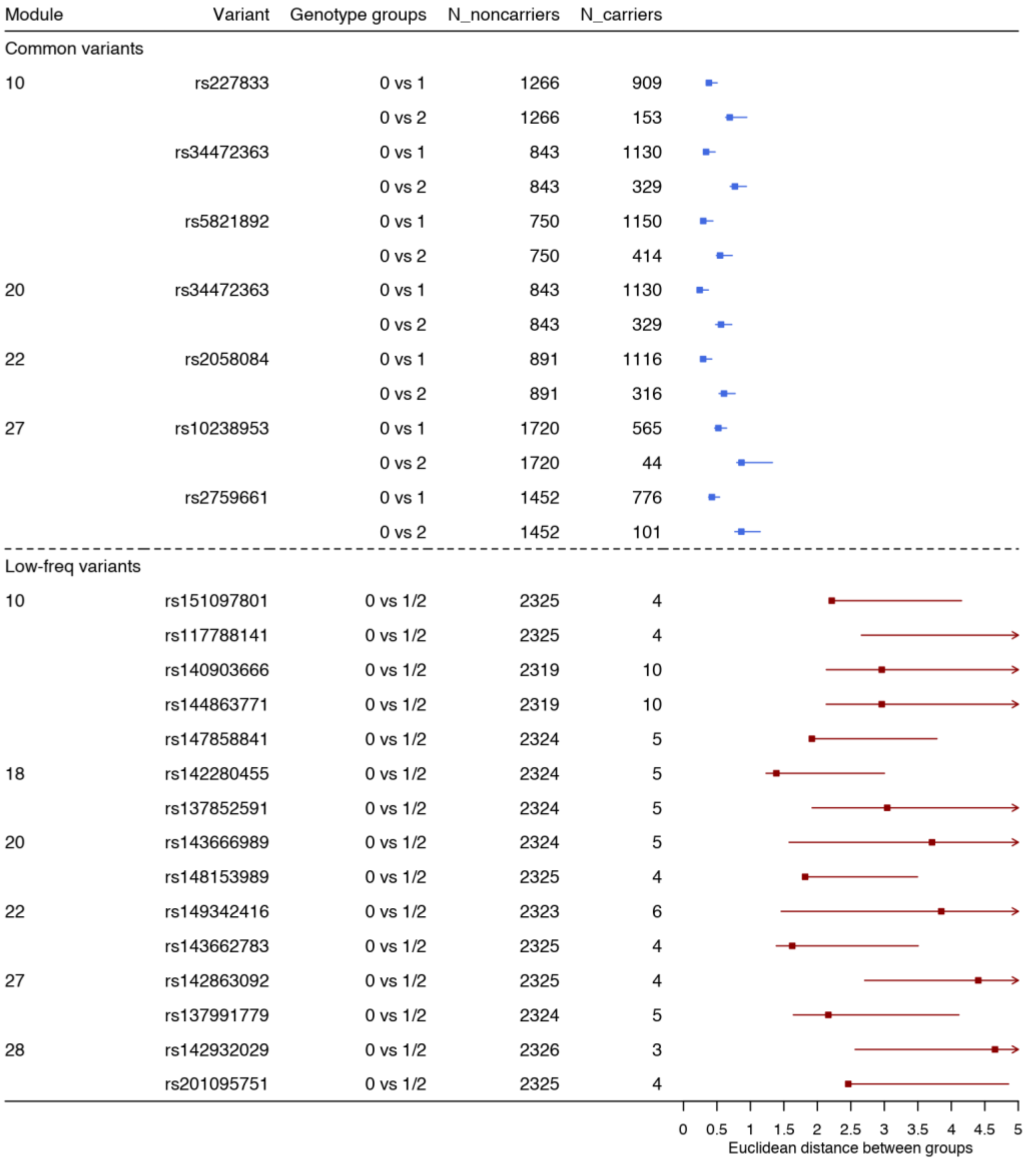

| Module | Variant | Genotype groups | N_noncarriers | N_carriers |
|---|---|---|---|---|
| Common variants | | | | |
| 10 | rs227833 | 0 vs 1 | 1266 | 909 |
| | | 0 vs 2 | 1266 | 153 |
| | rs34472363 | 0 vs 1 | 843 | 1130 |
| | | 0 vs 2 | 843 | 329 |
| | rs5821892 | 0 vs 1 | 750 | 1150 |
| | | 0 vs 2 | 750 | 414 |
| 20 | rs34472363 | 0 vs 1 | 843 | 1130 |
| | | 0 vs 2 | 843 | 329 |
| 22 | rs2058084 | 0 vs 1 | 891 | 1116 |
| | | 0 vs 2 | 891 | 316 |
| 27 | rs10238953 | 0 vs 1 | 1720 | 565 |
| | | 0 vs 2 | 1720 | 44 |
| | rs2759661 | 0 vs 1 | 1452 | 776 |
| | | 0 vs 2 | 1452 | 101 |
| Low-freq variants | | | | |
| 10 | rs151097801 | 0 vs 1/2 | 2325 | 4 |
| | rs117788141 | 0 vs 1/2 | 2325 | 4 |
| | rs140903666 | 0 vs 1/2 | 2319 | 10 |
| | rs144863771 | 0 vs 1/2 | 2319 | 10 |
| | rs147858841 | 0 vs 1/2 | 2324 | 5 |
| 18 | rs142280455 | 0 vs 1/2 | 2324 | 5 |
| | rs137852591 | 0 vs 1/2 | 2324 | 5 |
| 20 | rs143666989 | 0 vs 1/2 | 2324 | 5 |
| | rs148153989 | 0 vs 1/2 | 2325 | 4 |
| 22 | rs149342416 | 0 vs 1/2 | 2323 | 6 |
| | rs143662783 | 0 vs 1/2 | 2325 | 4 |
| 27 | rs142863092 | 0 vs 1/2 | 2325 | 4 |
| | rs137991779 | 0 vs 1/2 | 2324 | 5 |
| 28 | rs142932029 | 0 vs 1/2 | 2326 | 3 |
| | rs201095751 | 0 vs 1/2 | 2325 | 4 |